ELLIPSOMETRIC STUDY OF Sb DOPED ZnO THIN FILMS DEPOSITED BY MAGNETRON CO-SPUTTERING METHOD

A. M. AL-BARADI[a], M. M. ABD EL-RAHEEM[a,b], H. I. ALKHAMMASH[a], F. ABDEL- WAHAB[a,c] , S. ALOMAIRY[a], M. A. ALHARBI[a] , EL-NAGGAR[d,e], A. A. ALBASSAM[d].

[a]*Department of physics, Faculty of Science, Taif University, Taif 888, KSA*
[b]*Department of physics, Faculty of Science, Sohag University, Sohag 82524, Egypt*
[c]*Department of physics, Faculty of Science, Aswan University, Aswan. Egypt*
[d]*Research chair of Exploitation of Renewable Energy Applications in Saudi Arabia, Physics & Astronomy Dept., College of Science, King Saud University, P.0.Box 2455, Riyadh 11451, KSA*
[e]*Physics department, Faculty of Science, Ain Shams University, Abassia, Cairo 11566, Egypt.*

In this study, thin films of antimony zinc oxide were prepared at room temperature using the magnetron co-sputtering technique. The power on Sb target was varied from zero watt to 20 watt, whereas the power on ZnO target was fixed at 100 watt. The contents of the constituents of Sb-ZnO was determined using energy dispersive X-ray (EDX) spectrometry. The structural quality and surface morphology of the films were studied using X-ray diffraction (XRD) and scanning electron microscopy (SEM), respectively. Spectroscopic ellipsometery was used to determine the structural and optical properties of polycrystalline Sb-ZnO thin films under test. To evaluate ellipsometric measurements the Tauc-Lorenz model was used. The ellipsometric investigation showed, that the optical band gap decreased with increasing the ratio of Sb. The refractive index showed a decrease with increasing the content of Sb in addition to its behavior as a normal dispersion.

(Received April 2, 2017; Accepted July 24, 2017)

Keywords: Sb-ZnO; Co-sputtering; Ellipsometric measurements; Tauc-Lorentz model; optical constants

1. Introduction

Recently, semiconductors oxides with wide-gap have attracted excessive interests, due to their various applications in optics and optoelectronics. ZnO considered as one of the most promising materials, it has direct wide band gap of 3.3 eV and a large exciton binding energy of 60 meV. In order to improve their physical properties it is necessary to dope ZnO thin films. Doping with Cu, Al, In and Ga produced highly conductive n-type ZnO [1–4]]. In addition, doping ZnO with Sb creates p-type ZnO [5]. Several techniques have been used to get Sb doped ZnO thin films, such as spin coating [6], pulsed laser deposition [7], chemical vapor deposition [8], RF sputtering [9], hydrothermal process [10], sol–gel [11].

Knowledge about spectral dependence of optical parameters such as dielectric constants, refractive index, absorption coefficient etc. are necessary in the classification of materials which are used in the manufacture of opto-electronic devices. These parameters are frequently verified by spectrophotometry, prism-coupling technique, and ellipsometry SE. It is proffered to use the ellipsometric method because it is nondestructive, fast, very sensitive to the occurrence of surface inclusions and give good accuracy for determination of the optical parameters and thickness of thin layers in comparison with the others [12–15].

*Corresponding author: thobyani@yahoo.com

In order to estimate the optical parameters, spectroscopic ellipsometry data needs an accurate representation of film's optical response. Several optical models have been proposed to extract the precise optical properties and thickness of films.

In the present work, we first grew undpoed and Sb doped ZnO thin films by magnetron co-sputtering technique. The effect of Sb dopant on structural, morphological, optical properties has been studied using XRD, SEM, and ellipsometric method, respectively.

2. Experimental technique

2.1. Preparation of the thin films

Zn-SbO thin films in this study were deposited on pre-cleaned glass substrates using UNIVEX 350 SPUTTERING UNIT with DC POWER MODEL Turbo drive TD20classic (Leybold) and thickness monitor model INFICON AQM 160. The ceramic ZnO and Sb targets are obtained from Cathay Advanced Materials Limited Company as a sputtering source. The sputtering chamber was evacuated to a base pressure of $2x10^{-6}$ torr and was back filled with pure argon up to the sputtering pressure of $2x10^{-2}$ torr and the sputtering pressure was maintained constant throughout the coating. Prior to deposition, the substrates were cleaned using a 10% by volume solution of hydrofluoric acid followed by rinse in de-ionized water. The target substrate distance was kept 10 cm with an angle 65º. The standard cubic centimeter per minute (sccm) was kept at 20 cm^3/min with substrate rotation 2 rpm. The power on ZnO target was kept constant of 100 W, and the power on Sb target was changed from 0 up to 20 W. The rate of deposition was 2 nm/min.

2.2. Characterization of the films

X-ray diffraction (XRD) patterns were recorded using Philips X-ray diffractometer model X' Pert with Cu Kα (1.5406 Ao) radiation operated at 40 kV and 25mA.The scanning speed of the diffraction patterns were 2 deg/min.The surface micrograph was examined using scanning electron microscope (SEM) (Hitachi S4700). Energy dispersive X-ray EDX analysis was used to determine the content of Sb, Zn, and O_2 components. Optical measurements were accomplished using Woollam Variable Angle Ellipsometry VASE in the visible and near-UV region of the spectrum at wavelength 245nm and 1689 nm, step of 1 59 nm, at 55 º, 65 º and 75ºangle of incidence. Data analysis was performed with the WVASE32 software [16]. In the present study only the mean square error (MSE) is used to be an index to demonstrate the difference between the experimental results and the model expected data. The minimum value of MSE the better fitting is obtained.

3. Results and discussions

3.1. X-ray, EDX and SEM analysis,

X-ray diffraction patterns for Sb-ZnO thin films deposited under the powers 0 and 10 W on Sb target revealing polycrystalline nature as shown in Fig.1 Strong ZnO (002) diffraction peak belongs to both films at 33.5^o and at 33.88^o respectively which are very close to the reported diffraction peak [17]. It is observed that the peak related to 0 W power is higher than that of the 10 W power, it tacit that the lattice constant c of the lower power is smaller than that of the higher one. In fact the result shows that the increase of the power on Sb target causes reduction of the growth of ZnO thin films in (002) crystallographic orientation. The second highest peak is located at 34.55^o and 35.8^o for 0 W and 10 W respectively which are close to the reported one of ZnO diffraction [17]. Smaller peaks are observed at 35.5^o and at 72.57^o of the plane (004) belonging to ZnO are consistent with the reported one [17]. In addition, larger peak is observed at 25^o of plane (310) belonging to ZnO which agree with that reported by Jimenez et.al [18]. The increasing the power on Sb target results in slight shift of the peaks toward longer incident angle (2θ). The shift of the peak towards longer diffraction angle in the present work may be owed to the increase of tensile stress in the film [19].

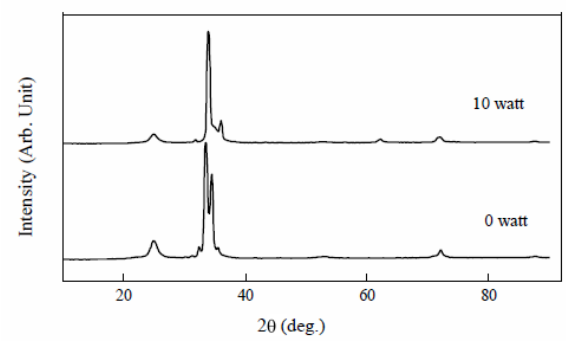

Fig. 1. X-ray diffraction patterns of Sb-ZnO thin films prepared under different power on Sb target

The effect of increasing the power on Sb on the surface morphology of the as-deposited Sb-ZnO thin films is observed in figure (2). Zinc oxide film showed inhomogeneous film of observable pore Fig.(2-a). On the other hand, increasing the power on Sb target (increasing the content of Sb) results in more tighter crystal grain Fig. (2-b,c) indicating that the grain size and density decreased, this means that Sb inhibits grain growth of ZnO.

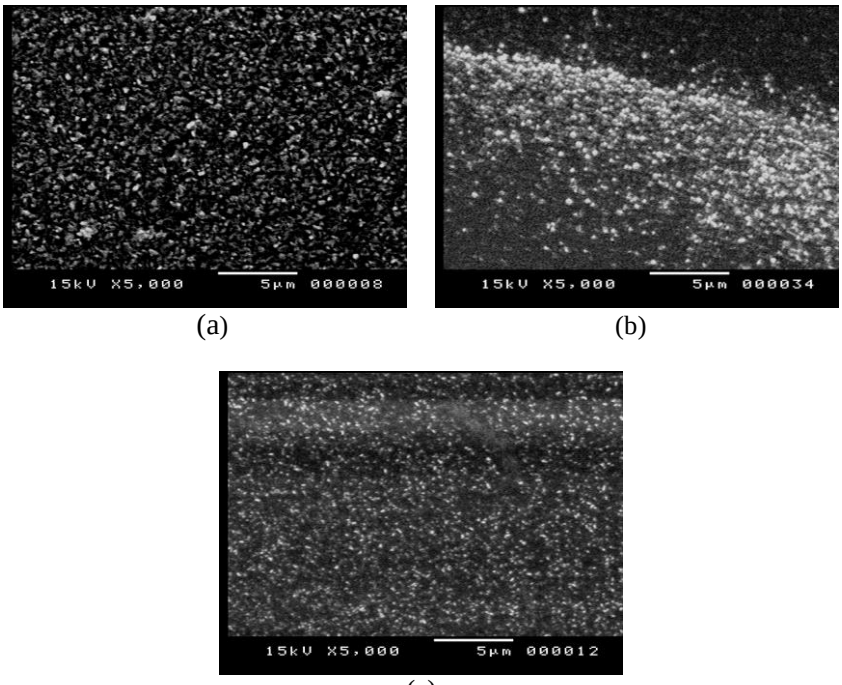

(a) (b)

(c)

Fig. 2. Surface micrograph of (a)ZnO film (b) Sb-ZnO (10 w on Sb target) (c) Sb-ZnO (20 w on Sb target)

The successful incorporation of Sb in the ZnO lattice was confirmed by EDX analysis. The ratios of Sb and ZnO in the prepared films under different power on Sb target (0.0 W, 10 W and 20 W) with constant power on ZnO (100 W) are determined using energy dispersive X-ray (EDX) spectrometry as shown in Fig.(3). Fig. (3–a) shows that the mass ratios of oxygen and zinc oxide are 20 and 80 respectively; besides, there is no component of antimony. Power of 10 W on Sb target results in the ratios 18.68, 78.82, 2.49 for O_2, Zn, and Sb respectively as revealed in Fig.(3-b). Raising the power up to 20 W on Sb target results in the ratios 18.87, 73.89, 7.24 for O_2,

Zn, and Sb respectively as demonstrated in Fig.(3-c). The EDX analysis reveals that increasing power on Sb target results in increasing the content of Sb in the matrix

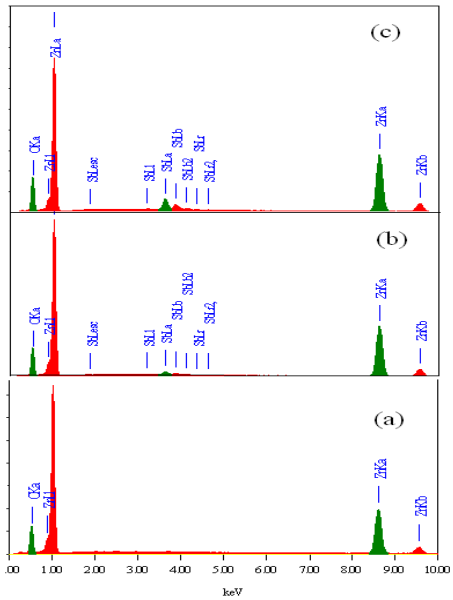

Fig. 3. EDX spectra of Sb-ZnO for (a): zero W power on Sb target.(b): 10 W power on Sb target. (c): 20 W power on Sb target.

3.2. Ellipsometric analysis

Ellipsometric technique is an indirect one and the information is obtained from optical models. As it is known that ellipsometer measures the change in the polarization state of the light beam after being reflection from a surface. The parameters measured with this technique are the ellipsometric angles defined asψandΔ. The $\psi$and Δ spectra of the ZnO-Sb samples (data points) are shown in Fig. 4a and b, respectively. For better clarity, only the spectra obtained at an angle of incidence of 55° are shown.

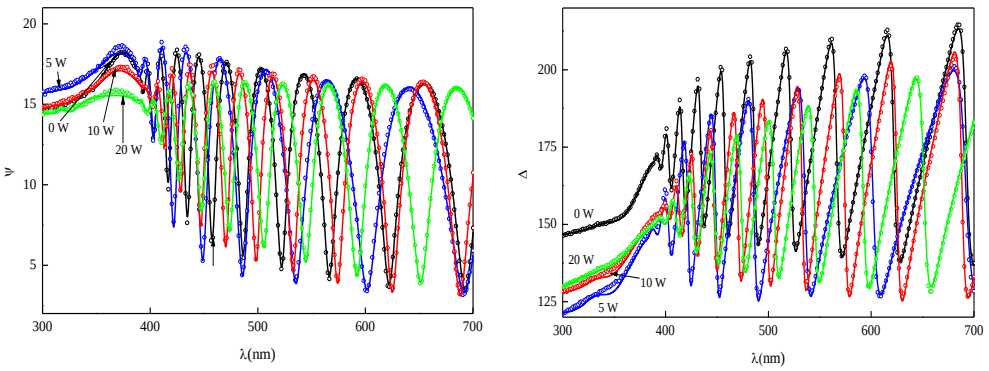

(a) (b)

Fig. 4. Experimental data of (a)Ψand (b) Δ spectra for Sb-ZnO thin films deposited under different power at an angle of incidenceof 55° (open circles). The solid curves represents best fit of linear combination of TL model.

The $\psi$and $\Delta$are related to the change of the polarization state through the Fresnel complex reflection coefficients by means of ellipsometric fundamental equation [20]:

$$\rho = \frac{r_p}{r_s} = \tan\psi \exp(i\Delta) \quad (1)$$

since r_s and r_p are the complex reflection coefficients perpendicular and parallel to the plane of incidence and ρ is the change in the polarization state.Since the determination of the dielectric constant is the key to understanding the optical responses of the samples, we report the parameters obtained by SE, which are conventionally given fromρ. The samples were considered as isotropic optical medium allowing to calculatethe so-called pseudo-dielectric function directlyfrom ρ [15]:

$$\langle\varepsilon\rangle = \varepsilon_1 + i\varepsilon_2 = \varepsilon_a \left[\left(\frac{1-\rho}{1+\rho}\right)^2 sin^2\Phi_a + cos^2\Phi_a\right] tan^2\Phi_a \quad (2)$$

Where Φ_a angle of incidence and ε_a is the ambient dielectric function which equal unity.

The pseudo-dielectric function extracted from $\psi$and Δ acquired at 55 º, 65 º and 75ºforSb-ZnO samples is shown in Fig. 5 (a-d). A main features observed from this figures is location of broad peak at about 4 eV. Note that, there are no effect of Sbcontent on the position of this peak.However with increasing the Sb content the values of ε_1 and ε_2 decreases. Also at higher energies, the values dielectric starts to increase, this is suggested the presence of other peak beyond our measurements. The occurrence of more than one peak in $\langle\varepsilon_2(E)\rangle$ is a typical behavior of amorphous chalcogenide semiconductors [21-23]. In contrast, a single peaked $\langle\varepsilon_2(E)\rangle$ spectrum has been observed in amorphous tetrahedrally bonded semiconductors [24-26] (R). Thus, the data are fit to a summation (linear combination) of several mathematical dispersion functions describing the dielectric function over the measured spectral range. Oscillators functions used for this work include the Tauc–Lorentz [27, 28] for fitting the fundamental band gap and higher energies in the ultraviolet. The imaginary part of the dielectric function has the following expressions.

$$\varepsilon_{2TL}(E) = \frac{\left(E-E_g\right)^2}{E^2} \frac{AE_0CE}{\left(E^2-E_0^2\right)^2+C^2E^2}, \qquad E > E_g \quad (3)$$

$$\varepsilon_{2TL}(E) = 0, \qquad E \le E_g \quad (4)$$

The real part of the dielectric function ε_{1TL} is calculated by the KK integration formula:

$$\varepsilon_{1TL}(E) = \varepsilon_1(\infty) + \frac{2P}{\pi}\int_{E_g}^{\infty} \frac{\xi\varepsilon_2(\xi)}{\xi^2-E^2} d\xi \ , \quad (5)$$

where A is the amplitude (oscillator strength), E_0 is the peak transition energy, C is the broadening term, and E_g is the optical energy band gap. For the real part ε_1, $\varepsilon_1(\infty)$ is a fitting constant to prevent ε_1 from converging to zero at energies below the band gap and P stands for the Cauchy principal part of the integral.

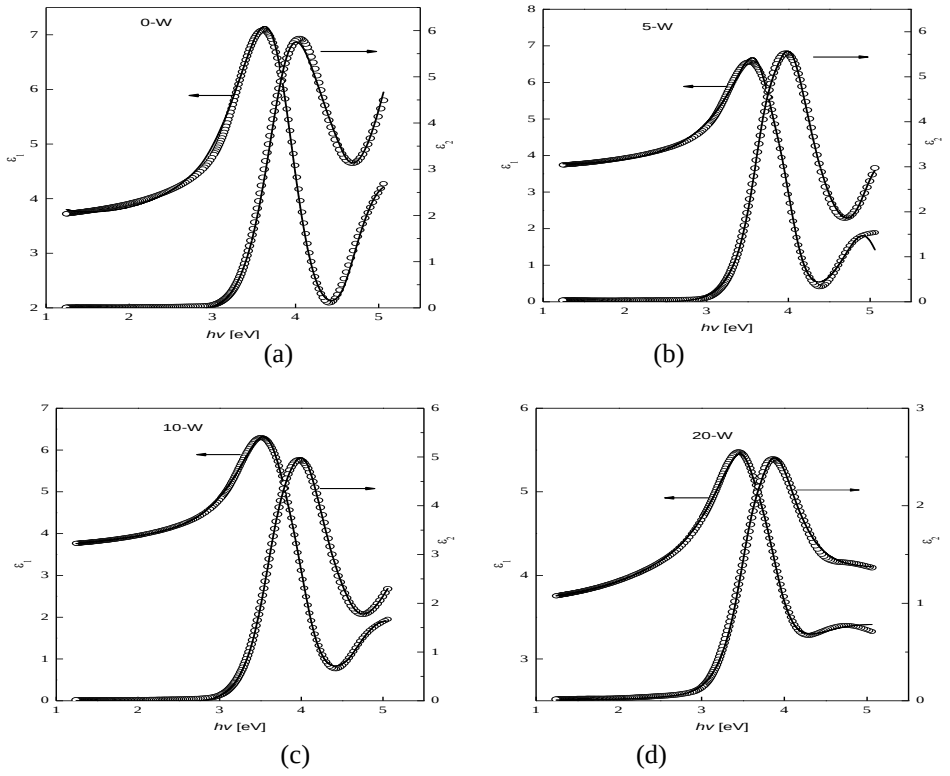

Fig. 5. Experimental data (open circles) of real (ε_1)and imaginary (ε_2)parts of the pseudodielectricfunction for Zn-SbO thin films with (a) 0 W, (b) 5 W, (c) 10 W, and (d) 20 W (b). the solid curves are calculated according to TL.

The comparison of experimental data for samples Sb-ZnO and modeled pseudo dielectric functions according to TL model(solid lines) were depicted in Fig. (5a & d) respectively. Note that the fitting procedure based on four layers system ambient/roughness/ thin film/glass substrate. Plausible agreement between the experimental data and the data modeled by the linear combination of TL oscillators is seen in the entire measured spectral region. The estimated parameters of TL model are scheduled in Table 1 as well as Sb-ZnO thin films thicknesses and roughness. In Table 1 the values of parameter χ are also introduced. The χ values enable us to judge the quality of the corresponding fits.

Table 1. Ellipsometic parameters of Sb-ZnO thin films

	0	5	10	20
χ	2.6	2.9	2.03	3.8
roughness(nm)	6.16 ± 0.306	19.07± 0.507	17.88± 0.472	20.14 ± 2.3
Thickness (nm)	1539 ± 3.26	1169 ± 4.2	1727 ± 6.4	1631 ± 24.02
A_1	874 ± 964.3	207.8± 57.48	299.6 ± 187	26.87± 16.98
C_1	2.812 ± 2.04	1.23 ± 0.224	2.01 ± 0.779	4.66 ± 2.29
E_{o1}	4.808±0.827	5.04 ± 0.052	4.86 ± 0.35	5.006 ± 0.26
E_{g1}	4.57 ± 0.031	4.51 ± 0.033	4.58 ± 0.031	2.94 ± 0.35
A_2	78.7 ± 2.16	25.23 ± 4.38	18.65 ± 6.61	14.53 ± 2.87
C_2	0.958±0.006	0.628±0.038	0.697±0.038	0.724 ± 0.03
E_{o2}	3.874±0.005	4.02±0.0095	4.029±0.011	3.85 ± 0.01
E_{g2}	2.889±0.012	2.82 ± 0.177	2.713 ± 0.28	2.702 ± 0.09
A_3	-------	20.58 ± 4.09	26.5 ± 4.86	0.399 ± 0.11
C_3	-------	0.601 ± 0.04	0.711± 0.027	0.492±0.016
E_{o3}	-------	3.71 ± 0.014	3.71 ± 0.016	3.593±0.008
E_{g3}	-------	2.605± 0.058	2.7 ± 0.107	2.707±0.345

After the estimation of $\varepsilon_1(E)$ and $\varepsilon_2(E)$ by fitting experimental data, refractive index $n(E)$ and extinction coefficient $k(E)$ dispersion can be considered as

$$n(E) = \left\{\left[(\varepsilon_1^2 + \varepsilon_2^2)^{1/2} + \varepsilon_1\right]/2\right\}^{1/2} \quad (6)$$

$$k(E) = \left\{\left[(\varepsilon_1^2 + \varepsilon_2^2)^{1/2} - \varepsilon_1\right]/2\right\}^{1/2} \quad (7)$$

The spectral dependences of both $n(E)$ and $k(E)$ of the Sb-ZnO films are depicted in Fig. (6 a & b). One can note that the refractive index n spectra can be divided into three region. First in the ultraviolet region *n* decreases with increasing the wavelength and go through a minimum at about 275 nm for all samples except 20 W. second, between 330 and 450 nm,*n*decrease with the increasing Sb content as will as with increasing wavelength and experience a maximum value. The peak values shift toward higher wavelength with increasing Sb content. Third region above 450 nm, *n* behaves as normal dispersion and no effect for Sb content. On the other hand, k behaves similar to n.

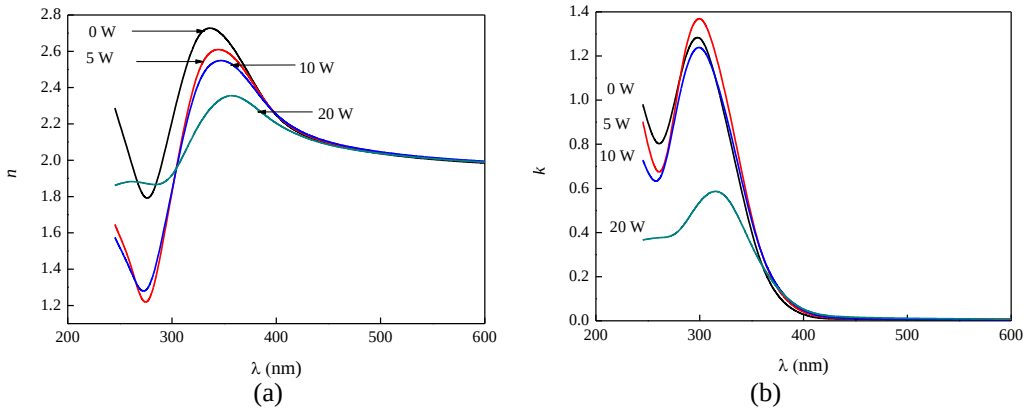

Figs. 6. Refractive indices(a) and extinction coefficients (b) Zn-SbO thin films

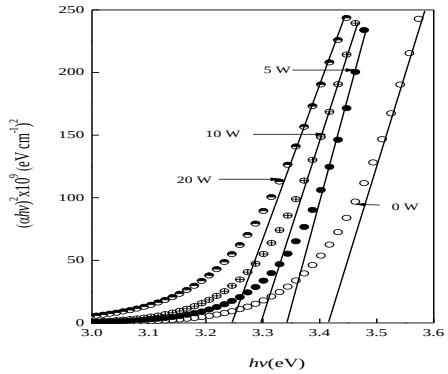

Fig. 7. Plots of $(\alpha h\nu)^2$ versus photon energy for Sb-ZnO thin films deposited under different powers on Sb target.

The absorption coefficient α is computed from the well-known equation, $\alpha = 4\pi k/\lambda$. The fundamental absorption edge in the a large amount semiconductors follows an exponential law. Above the exponential tail, the absorption coefficient has been accounted to obey the following equation:

$$\alpha h\nu = b\left(E - E_g\right)^r \quad (8)$$

where b is a constant, and *r* is an exponent, and its values depend on the nature of electronic transition responsible for the absorption. It should be mentioned that r values can be assumed to be 1/2, 3/2, 2 and 3, for allowed direct, for forbidden direct, allowed indirect and forbidden indirect transition, respectively. Fig. (7) shows the $(\alpha h\nu)^2$ versus $h\nu$ plot. For each films, the value of Eg has been calculated by extrapolating the linear portion of the plots of $(\alpha h\nu)^{1/2}$ versus the photon energy ($h\nu$) to $\alpha h\nu = 0$. The corresponding band gaps of Sb-ZnO films prepared at Sb power 0.0, 5, 10, and 20 w are 3.42, 3.34, 3.30 and 3.25 eVeV respectively. The slight decrease of the optical gap with increasing the doping content of Sb can be owed to the existence of Sb defects in the optical gap.

4. Conclusions

A Sb-ZnO thin films have been deposited on a glass substrate by magnetron co-sputtering technique at different power on Sb target with fixed power on ZnO target. These films are investigated by XRD, SEM, and EDX revealing that the prepared films have polycrystalline structure.

The SE data were found to fit very well using linear combination of several Tauc-Lorenz model. Increasing the Sb content in the films under test resulted in a significant decrease in the value of Eg accompanied by decreasing in the magnitude of dielectric constants.

Acknowledgments

The project was financially supported by King Saud University, Vice Deanship of research chairs.

References

[1] H. Gong, J.Q. Hu, J.H. Wang, C.H. Ong, F.R. Zhu, Sensor. Actuat. B-Chem. **115**, 247 (2006).
[2] Y. Caglar, S. Ilican, M. Caglar, F. Yakuphanoglu, Spectrochim. Acta A **67**, 1113 (2007).
[3] M. Sahal, B. Hartiti, A. Ridah, M. Mollar, Afrique Science **02**, 245 (2006).
[4] L. Seung-Yup, P. Byung-Ok, Thin Solid Films **484**, 184 (2005).
[5] K. Eun Lee, M. Wang, E. Jung Kim, S. Hong Hahn, Curr. Appl. Phys. **9**, 683 (2009).
[6] H. Benelmadjat, N. Touka, B. Harieche, B. Boudine, O. Halimi, M. Sebais, Opt.Mater. **32**, 764 (2010).
[7] X.Q. Gu, L.P. Zhu, J. Mater. Sci.: Mater. Electron. **24**, 1976 (2013).
[8] Y. Yang, J. Qi, Q. Liao, Y. Zhang, L. Tang, Z. Qin, J. Phys. Chem. C **112**, 17916 (2008).
[9] J. Ayres de Campos, T. Viseu, A. G. Rolo, N.P. Barradas, E. Alves T. de Lacerda-Arôso, M.F. Cerqueira, J.Nanoscience and Nanotechnology **10**, 2620 (2010).
[10] A. Escobedo-Morales, U. Pal, Curr. Appl. Phys. **11**, 525 (2011).
[11] F Al-juaid, A Merazga, A Al-Baradi, F Abdel-wahab, Solid-State Electronics **87**, 98 (2013).
[12] R. V. A. Azzam and N. M. Bashara, Ellipsometry and Polarized Light, chapter 4, North-Holland, Amsterdam, The Netherlands, 1977.
[13] L. Ward, Journal of Physics D, **17(**9), 1781 (1984).
[14] K. Vedam, Thin Solid Films, **313-314**, 1 (1998).
[15] D. E. Aspnes, Thin Solid Films, **455-456**, 3 (2004).
[16] Guide to Using WVASE 32, J.A. Woollam Co., Inc., Lincoln NE.
[17] Hong Ming Zhou, Dan-Qing Yi, Zhi-Ming Yu, Lai-Rong Xiao, Jian Li, Thin Solid **515**, 6909 (2007).
[18]A. E. Jimenez-Gonzalez, J. A. S. Urueta, R. Stuarez-Parra, J. Crys. Growth **192**, 430 (1998).
[19] C. Privato, A. Antonaia, M. L. Addolnizio, A. Di Nocera, S. GLoreti, E. Terzini, Proceedings of the 13th European Photovoltaic Solar Energy Conference, Nice, France 1995, P1623

[20] C.M. Herzinger, P.G. Synder, B. Johs, J.A. Woollam, J. Appl. Phys. **77**, 1995 (1715).
[21] S. Kumar, D. K. Pandya, L. Chopra, Thin Solid Films **164**, 51 (1988).
[22] T. Ojima, S. Adachi, J. Appl. Phys. **82**, 3105 (1997).
[23] F Abdel-Wahab, A Merazga, MS Rasheedy, AA Montaser, Optik **127**, 3871 (2016).
[24] T. Yamaguchi, Y. Kaneko, A.H. Jayatissa, M. Aoyama, Thin Solid Films **279**, 174 (1996).
[25] T. Berlind, A. Furlan, Zs. Czigany, J. Neidhardt, L. Hultman, H. Arwin Thin Solid Films **517**, 6652 (2009)
[26] E. S. M. Goh, T. P. Chen, C. Q. Sun, Y. C. Liu , J. App. Phys **107**, 024305 (2010).
[27] G. E. Jellison, Jr. and F. A. Modine, Appl. Phys. Lett. **69**, 371 (1996).
[28] G. E. Jellison, Jr. and F. A. Modine, Appl. Phys. Lett. **69**, 2137 (1996).